



Investigation of shrinkage behavior of Ni–Fe bimetallic anode tube support and the densification of electrolyte using co-sintering temperature

Bo Liang^{a,*}, Toshio Suzuki^{a,1}, Koichi Hamamoto^{a,1}, Toshiaki Yamaguchi^{a,1}, Yoshinobu Fujishiro^{a,1}, Masanobu Awano^{a,1}, Brian J. Ingram^b, John David Cater^b

^a National Institute of Advanced Industrial Science and Technology, Shimo-shidami, Moriyama-ku, Nagoya 463-8560, Japan

^b Chemical Science and Engineering Division, Argon National Laboratory, 9700 South Cass-Avenue, Bldg. 205, Argonne, IL 60439-4873, United States

ARTICLE INFO

Article history:

Received 24 February 2011

Received in revised form 25 April 2011

Accepted 16 May 2011

Available online 6 July 2011

Keywords:

Fuel cell
Anode–electrolyte
Co-sintering
Porosity
Densification

ABSTRACT

NiO–Fe₂O₃/gadolinium-doped CeO₂ (GDC), NiO–Fe₂O₃/yttria-stabilized ZrO₂ (YSZ) anode supported fuel cells were fabricated at co-sintering temperatures of anode–electrolyte from 1250 °C to 1400 °C. The volumetric shrinkage of the anode–electrolytes and the porosity of the anode tube were studied systematically at different temperatures. 1300 °C is the marginal temperature to obtain sufficient electrocatalytic activity of electrodes, and a higher temperature is needed to suppress gas leakage through the scandia-stabilized zirconia (ScSZ) electrolyte. At each co-sintering temperature from 1250 °C to 1400 °C, the porosity of NiO–Fe₂O₃/GDC anode tubes is nearly 10% higher than that of NiO–Fe₂O₃/YSZ anode tubes. SEM results exhibited the anode-supported electrolyte tends to be more dense as co-sintering temperature increasing to 1400 °C from 1250 °C. However, the high co-sintering temperature of 1400 °C will result in low porosity of anode which negatively affected the power density.

© 2011 Elsevier B.V. All rights reserved.

1. Introduction

Solid oxide fuel cells (SOFCs) have been recognized as a keystone of the future eco-energy economy, especially for local and emergency power generation, [1–4] due to their high energy conversion efficiency, fuel flexibility and low environmental pollution [5–8]. Among all types of SOFCs, micro tubular design has been intensively studied due to its high volumetric power density, [9–11] and could endure thermal stress caused by rapid heating up to the operating temperature. [12–18] Furthermore, anode tube supported design makes feasible one-step sintering of anode–electrolyte bi-layers. A high co-sintering temperature up to 1400 °C tends to give a crack-free and dense electrolyte layer, which is preferred to increase the cell open circuit voltage (OCV). However, the porosity of the anode tube will decrease at high co-sintering temperature, which resulted in poor output power density. It is because large amount of pores in anode shrink more at high co-sintering temperature than at low temperature. On one hand, those pores provide place where fuel gases diffused. On the other hand, a large active surface area of catalysts will increase the rate of the electrochemical reaction. So, in a

co-sintering process of anode supported electrolyte, obtaining both dense electrolyte and high porosity of anode tube is quite important to improve the fuel cell performance.

In this study, two kinds of tubular SOFCs were fabricated to investigate how the co-sintering temperature affected the shrinkage behavior of Ni–Fe bimetallic anode and the densification of electrolyte. The anode tubes consist of the conventional materials: NiO, Fe₂O₃, YSZ, and GDC, namely NiO–Fe₂O₃/GDC, NiO–Fe₂O₃/YSZ anode tubes. Ni–Fe bimetal was used because they show interesting improvement to anode tube [19–22]. After securely fabricating a very thin ScSZ electrolyte film on each of anode tubes, the densification behavior of the electrolyte layer at co-sintering temperatures from 1250 °C to 1400 °C was compared using field emission scanning electron microscopy (FE-SEM). The shrinkage degree of anode tube both in length and in diameter is presented at different temperatures. The corresponding OCV, I–V properties and impedance of each fuel cell were measured to investigate how the co-sintering temperature affected their values. The cell performance was discussed with the impedance results, the porosity of anode tube, together with FE-SEM images of the tubes and electrolyte.

2. Experimental

2.1. Description of the test cells

Two kinds of anode tubes (NiO–Fe₂O₃/YSZ and NiO–Fe₂O₃/GDC) were fabricated. In the case of NiO–Fe₂O₃/YSZ anode tubes, they were made by mixing of NiO and Fe₂O₃ powders (Ni:Fe is 9:1 by

* Corresponding author. Tel.: +81 52 7367581; fax: +81 52 736 7405.

E-mail addresses: boliang-riyou@aist.go.jp, basafan@gmail.com (B. Liang), toshio.suzuki@aist.go.jp (T. Suzuki), k-hamamoto@aist.go.jp (K. Hamamoto), tosiroy-yamaguchi@aist.go.jp (T. Yamaguchi), y-fujishiro@aist.go.jp (Y. Fujishiro), masa-awano@aist.go.jp (M. Awano), ingram@anl.gov (B.J. Ingram), jdcarter@anl.gov (J.D. Cater).

¹ Fax: +81 52 736 7405.

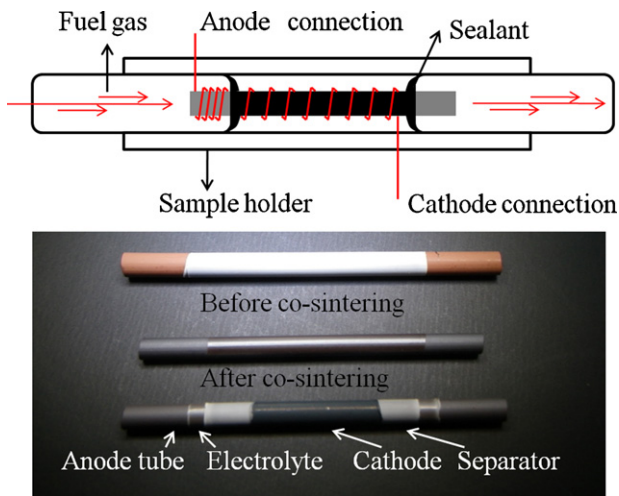


Fig. 1. Experimental apparatus for testing single tubular cell (top) and images of a Fe_2O_3 -containing SOFC (bottom).

mol), YSZ powder, poly methyl methacrylate beads (PMMA), and binder. These powders were mixed for 1 h by a mixer (5DMV-r). After adding proper amount of water, they were stirred for 30 min in a vacuum chamber. The mixture (clay) was aged for 15 h. Then, the tubes were extruded from a metal mold by using a piston cylinder type extruder. Using co-sintering process, a very thin ScSZ electrolyte around $5\ \mu\text{m}$ was securely fabricated on the anode tubes. In detail, an electrolyte layer was dip-coated on the anode tube using a ScSZ slurry. The coated tube was dried in air, then, the anode-electrolyte tubes were sintered at $1250\text{--}1400\ ^\circ\text{C}$ for 1 h in air. They were again dip-coated using a GDC slurry and sintered at $1200\ ^\circ\text{C}$. Next, the anode tubes with electrolyte (ScSZ) and interlayer (GDC) were dip-coated in cathode slurry. This cathode slurry consisted of $\text{La}_{0.6}\text{Sr}_{0.4}\text{Co}_{0.2}\text{Fe}_{0.8}\text{O}_{3-y}$ (LSCF) and GDC powders (weight ratio = 3:1) and organic ingredients. Organic ingredients were similar with those of the electrolyte slurry. After dip-coating the cathode slurry, the tubes were dried and sintered at $1050\ ^\circ\text{C}$ for 1 h to complete a cell [23]. Furthermore, $\text{NiO-Fe}_2\text{O}_3/\text{GDC}$ tubular cells were also prepared with the same weight ratio of anode components except replacing YSZ with GDC.

The diameter and length of anode tube before and after co-sintering were measured by digital vernier caliper to compare the shrinkage degree. The pores volume of anode tube sintering at different temperature was tested by mercury porosimeter. Table 1 provides the size of particles (YSZ, GDC, NiO, Fe_2O_3 , PMMA bead, ScSZ) used for the anode and electrolyte. The anode sintering behavior depends partly on the particle size of the NiO, and Fe_2O_3 , also on the particle size of the YSZ or GDC. Since the same amount of NiO, Fe_2O_3 and PMMA beads were added to YSZ or GDC tubes, the difference between the particle size of GDC (630 nm in diameter) and YSZ (22 nm in diameter) will help to understand the micro structure of the 2 types of anode-electrolyte.

2.2. Fuel cell measurements

The performance of the cell was investigated using an experimental apparatus as shown in Fig. 1. The cell was sealed at an alumina tube using a ceramic sealing paste. Ag wires were used for collecting current of the anode and cathode, which were both fixed by painting a colloidal silver paste. Diluted hydrogen (20% H_2 in Ar) was flowed inside of the tubular cell with a flow rate of $47\ \text{mL min}^{-1}$. Cathode side was open to the air. The size of the cell was about 1.8 mm in diameter, 30 mm in tube length, and 10 mm in cathode length. The active cell area is $0.5\text{--}0.6\ \text{cm}^2$ depending on the

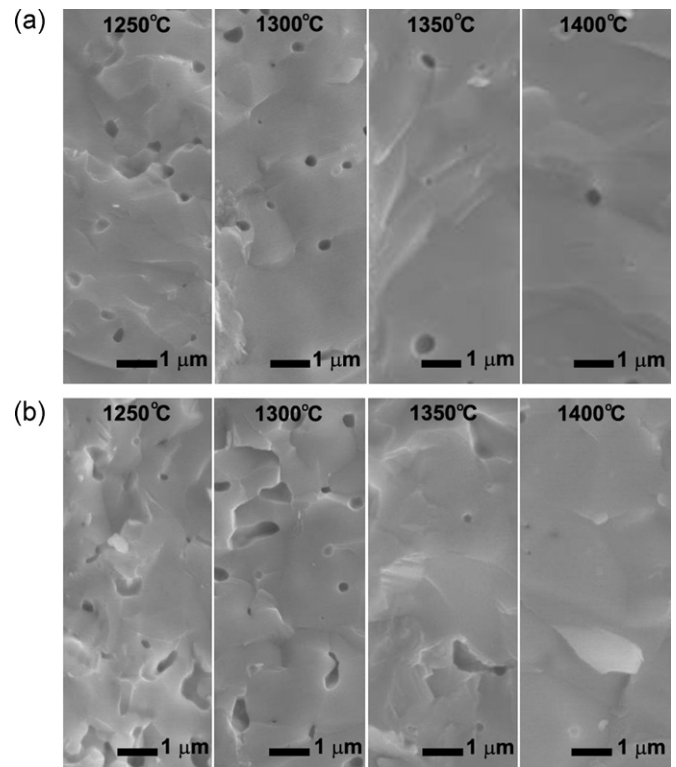


Fig. 2. Microstructure of the ScSZ electrolyte layer prepared at the sintering temperature of $1250\ ^\circ\text{C}$, $1300\ ^\circ\text{C}$, $1350\ ^\circ\text{C}$, and $1400\ ^\circ\text{C}$. $\text{NiO-Fe}_2\text{O}_3/\text{YSZ}$ anode tube supported (a), and $\text{NiO-Fe}_2\text{O}_3/\text{GDC}$ anode tube supported (b).

diameter shrinkage degree at different temperature. Open circuit voltage, I - V plots, and EIS plots were collected using a multichannel potentiostat (Solartron 1260 frequency response analyzer with a 1296 Interface) based on two chamber configuration.

3. Results and discussion

The densification behavior of the electrolyte layer was strongly related to the co-sintering temperature. Fig. 2 shows cross-sectional FE-SEM images of the $\sim 5\ \mu\text{m}$ thick electrolyte (ScSZ). It was initially coated on the four anode tubes and then sintered separately at temperatures between $1250\ ^\circ\text{C}$ and $1400\ ^\circ\text{C}$. As shown in Fig. 2, the microstructures of the electrolyte sintered at $1250\ ^\circ\text{C}$ and $1300\ ^\circ\text{C}$ included many pinholes. The higher the co-sintering temperature is, the fewer the pinholes inside the electrolyte layer exist. The trend can be observed in all Ni-Fe bimetal anode support tubular fuel cells in this study. The densification of the electrolyte deposited on the tubular support were also greatly affected by the shrinkage of the anode tube during the co-sintering process.[24] During the co-sintering process at temperatures up to $1300\ ^\circ\text{C}$, the densification of the electrolyte layer was assisted by a sintering stress caused by the shrinkage of tube support.

Fig. 3 shows shrinkage behaviors of various anode tubes as a function of co-sintering temperature. The densification of the as-sintered tubes started at a temperature lower than $1250\ ^\circ\text{C}$. As the temperature increasing, the tube shrank more both in diameter and length. The diameter at $1400\ ^\circ\text{C}$ is just about four fifth of its initial value. Also, the tube length of each the four anode tubes (prepared from $1250\ ^\circ\text{C}$ to $1400\ ^\circ\text{C}$) had a clear difference to that of the others. So, the tube shrinkage behavior of /GDC tubes or /YSZ tubes is closely related to the co-sintering temperature. Compared with the GDC-containing anode tubes, the YSZ-containing tubes apparently have large shrinkage degree at each temperature from $1250\ ^\circ\text{C}$ to $1400\ ^\circ\text{C}$. It is because the smaller starting particle size

Table 1
The particles size used in anode-electrolyte.

	ScSZ	YSZ	GDC	Fe ₂ O ₃	NiO	PMMA
D50 (μm)	0.62	0.022	0.63	0.05	0.1	5

of the YSZ powder (22 nm) than that of the GDC powder (660 nm), considering the same amount of PMMA was used.

Table 2 shows the porosity of anode tubes prepared at different temperature. In the case of NiO-Fe₂O₃/YSZ tubes, the value of porosity is 35.0% at 1250 °C, then decreased gradually to 20.0% at 1400 °C. In the case of NiO-Fe₂O₃/GDC tubes, the value of porosity at each temperature is higher than that of /YSZ tubes. Figs. 4 and 5 present the detail information of pores inside anode tubes. As shown in Fig. 4(a), the accumulated pore volume of NiO-Fe₂O₃/YSZ tubes decreased as the co-sintering temperature increasing. In details, it is nearly reach 0.1 cm³ g⁻¹ of accumulated pore volume at co-sintering temperature of 1250 °C, while the value decreases almost half to 0.042 cm³ g⁻¹ at 1400 °C. This is because the anode tube shrank more as temperature increasing. Furthermore, at temperature of 1250 °C, the volume of anode tube mainly consisted of the pores in diameter about 0.7 μm and the pores in diameter less than 0.5 μm. When the co-sintering temperature increased, the large pores increase their size, while small pores start to shrink. This shift of diameter distribution was shown in Fig. 4(b). At the co-sintering temperature of 1350 °C and 1400 °C, it clearly shows the largest one is about 1.2 μm in diameter, while it just 0.8 μm at 1250 °C. It is noted that the accumulated pore volume of GDC based tubes is higher than that of the YSZ based tubes. As shown in Figs. 4(b) and 5(b), the peak of real pore volume distribution for pore size in /GDC tubes is higher than that of its counterpart in /YSZ tubes at each sintering temperature. Because the pores provide place where fuel gases

diffused and a large surface area of catalyst particles will increase the rate of the electrochemical reaction, the microstructure of the anode tubes decides the output power density fuel cells (with the same electrolyte and cathode). So, the sintering temperature is quite important and requires significant attention. It deserves to note that the co-sintering temperature affected different on the densification of electrolyte and the porosity of anode tube.

Then, the open-circuit voltage of the two types of SOFCs sintered at temperatures from 1250 °C to 1400 °C was measured to investigate the relation between the OCV and the densification of the electrolyte. All samples were tested at 650 °C with a fuel gas (20% H₂ in Ar) flow rate of 50 mL. As can be seen in Fig. 6(a), the OCVs of the two types SOFCs decreased from 1.1 V to 1.0 V as the sintering temperature decreased from 1400 °C to 1250 °C. It is noted that NiO-Fe₂O₃/YSZ anode supported fuel cells almost generate the higher OCV at each co-sintering temperature than that of the NiO-Fe₂O₃/GDC tubes. At the same time, as shown in Fig. 3, their diameter shrinkage is also larger at each temperature compared with that of /GDC tubes. That is, the densification process of ScSZ electrolyte layer was enhanced by the degree of diameter shrinkage of anode tube, which results in obtaining higher OCV. As can be seen in Fig. 6(b), the OCVs of the cells are linearly increasing as the tube diameter shrinkage increasing.

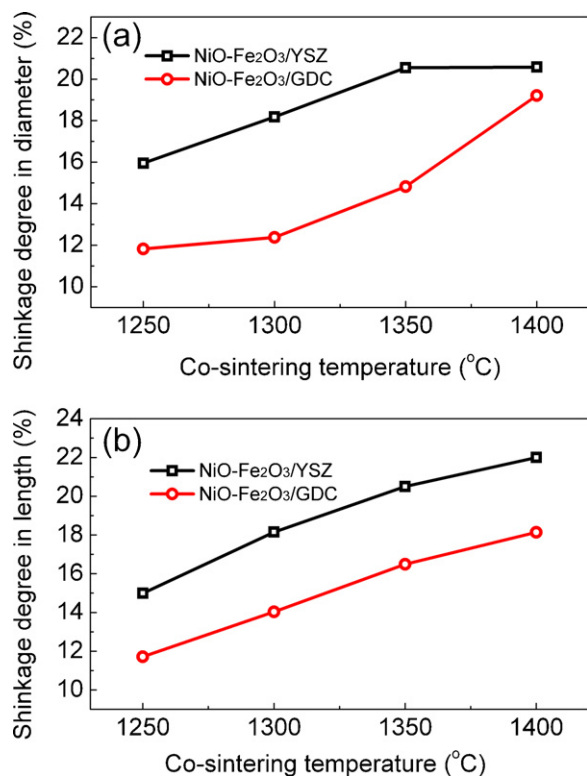


Fig. 3. The anode tube shrinkage behaviors as a function of co-sintering temperature. (a) The diameter shrinkage degree of anode tube, (b) The length shrinkage degree of anode tube.

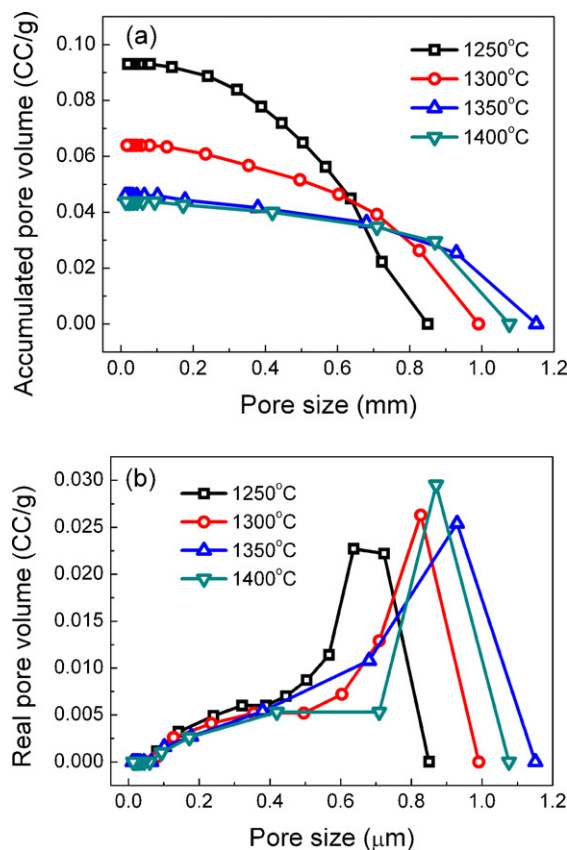


Fig. 4. Porous properties of NiO-Fe₂O₃/YSZ anode tube supported cells prepared at different sintering temperatures. (a) The cumulative pore volume of the anode tubes, and (b) volume fraction of the different-size pores.

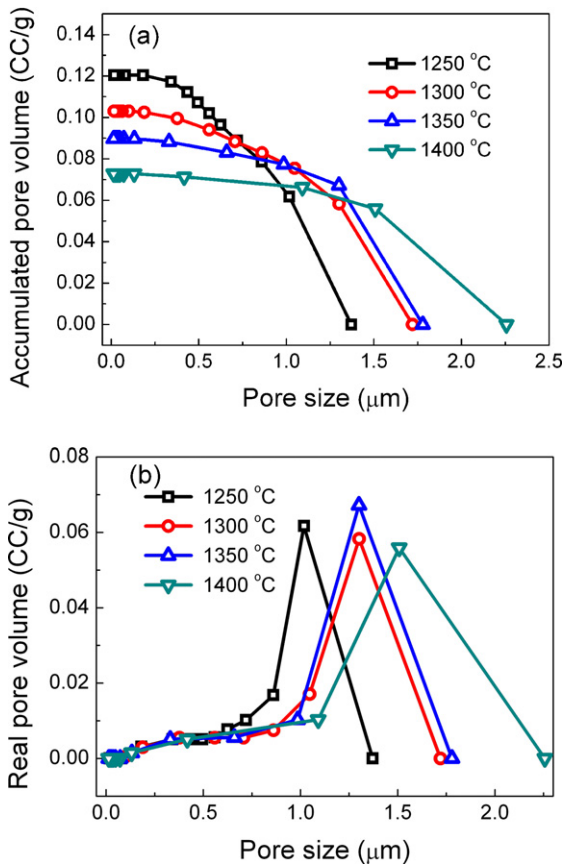


Fig. 5. Porous properties of NiO–Fe₂O₃/GDC anode tube supported cells prepared at different sintering temperatures. (a) The cumulative pore volume of the anode tubes, and (b) volume fraction of the different-size pores.

Theoretically, the Nernst voltage of the fuel cells can be calculated to compare with the measured OCV. It was helpful to decide whether the electrolyte sintered at 1400 °C is fully dense. When operating a tubular cell with H₂ as fuel, the Gibbs free energy of reaction are 399.312 kJ mol⁻¹ and 388.410 kJ mol⁻¹, respectively. The partial pressure of reactants and products can change in a fuel cell are by varying fuel utilization and pressurizing the anode or cathode. According the Nernst equation, in our experiments, it should generate 1.123 V between anode and cathode. The blue dotted lines show the calculated Nernst voltage value. However, the existence of the pinholes inside the electrolyte results in the leakage of O₂ or H₂ from one electrode to the other electrode. Thus, the OCV is less than 1 V at low co-sintering temperature. As shown in Fig. 2, the ScSZ electrolyte co-sintered lower than 1400 °C looks loose, and some pinholes can be clearly observed inside it. Even at 1400 °C, the electrolyte was not fully dense.

Unlike to generate high OCV at high co-sintering temperature, the cell performance prefer to be better at low co-sintering temperature, as shown in Fig. 7(a). It is different from the relation between densification of electrolyte and OCV, the porosity of anode tube plays more important role in the maximum output power density. Low co-sintering temperature resulted in high porosity of anode tubes and large active surface area of catalysts. As already shown in

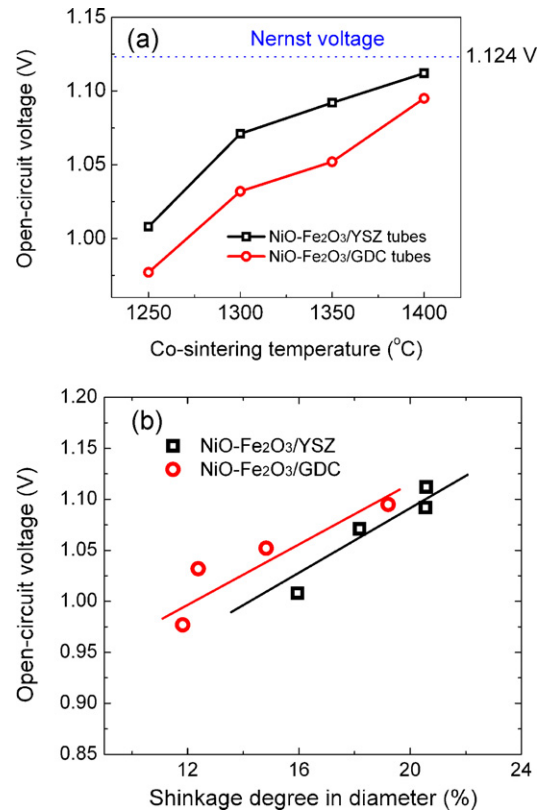


Fig. 6. (a) Open-circuit voltages of two types of micro-tubular SOFCs prepared at different temperature, (b) OCV changes as a function of diameter shrinkage of anode tubes.

Figs. 4 and 5, the lower the co-sintering temperature is, the higher the accumulated pore volume is. Fig. 7(b) and (c) shows the FE-SEM cross-sectional images of NiO–Fe₂O₃/YSZ and Ni–Fe₂O₃/GDC anode bodies co-sintered at 1250 °C and 1400 °C, respectively. As can be seen, the 5–10 μm pores existed in the anode due to the pore former (PMMA beads). Because the porosimeter seems not to be sensitive to those large pores, Figs. 4 and 5 did not show that range of the pore size. When co-sintering temperature increased, the /GDC and /YSZ particles coalesced with each other and became dense. That is, the active surface area of catalysts became small. Finally, it eventually will decrease the rate of electrochemical reaction. So, from the results of Figs. 4, 5 and 7, it can be concluded that the porosity of anode tube became worse as the co-sintering temperature increasing.

Considering both the densification of electrolyte and the porosity of anode tube, co-sintering temperature of 1300 °C is marginal temperature of tubular cell having a porous anode body with relatively dense electrolyte. The maximum power density at 1300 °C reaches 0.57 W cm⁻² for /GDC tube and 0.49 W cm⁻² for /YSZ tube, respectively. At sintering temperature of 1250 °C, although anode porosity was good, the densification of electrolyte did not finish. It resulted in gas leakage and relative lower OCV compare with that of at 1300 °C.

EIS plots are helpful to explain how co-sintering temperature affect the output power of the anode supported fuel cell. Fig. 8

Table 2
The total porosity of anode tube co-sintered at different temperature.

Co-sintering temperature	1250 °C	1300 °C	1350 °C	1400 °C
NiO–Fe ₂ O ₃ –YSZ	35.0%	26.7%	20.9%	20.0%
NiO–Fe ₂ O ₃ –GDC	43.2%	39.4%	36.3%	31.8%

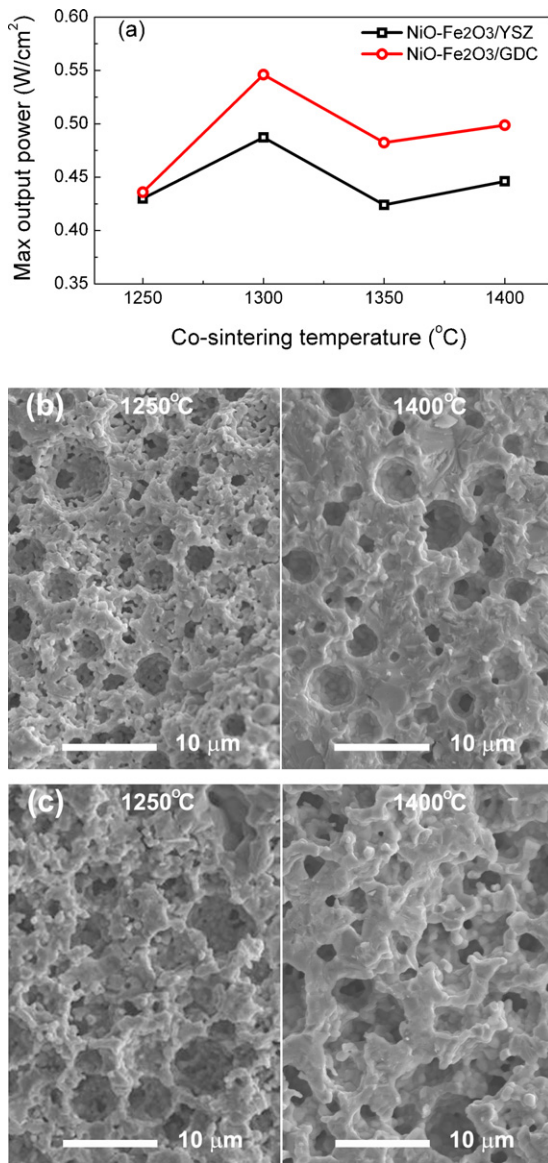


Fig. 7. (a) The maximum power density of Ni-Fe bimetallic fuel cells co-sintered at different temperature. The FE-SEM cross-sectional images of anode tubes made of (b) NiO-Fe₂O₃/YSZ, and (c) Ni-Fe₂O₃/GDC.

shows the impedance plots at each temperature of both two types of fuel cells. The testing condition is the same. All samples were tested at 650 °C with a fuel gas (20% H₂ in Ar) flow rate of 50 mL. There are two semi-circles for each impedance arc, which are usually interpreted as electrochemical reactions for the higher frequency arcs, and gas transport (gas diffusion) for the lower frequency arcs [25,26]. As can be seen in Fig. 8(a) and (b), two semi-circles for both the low frequency arc and the high frequency arc become bigger as the co-sintering temperature increasing. They contribute to the overpotential resistance in operating a fuel cell. Ohmic resistances determined from Fig. 8 were basically same about 0.35 Ωcm². The increasing of low frequency arcs at high co-sintering temperature of fuel cells is agree with the low porosity of anode tube. The higher co-sintering temperature is, the lower cumulated volume of pores inside anode provides for gas diffusing. At the same time, the increasing of high frequency arcs looks clearer than that of high frequency arcs, especially in /YSZ tubes. In the case of /YSZ tubes, the over potential resistance is about 0.4 Ωcm² of the cell prepared at 1400 °C and about 0.1 Ωcm²

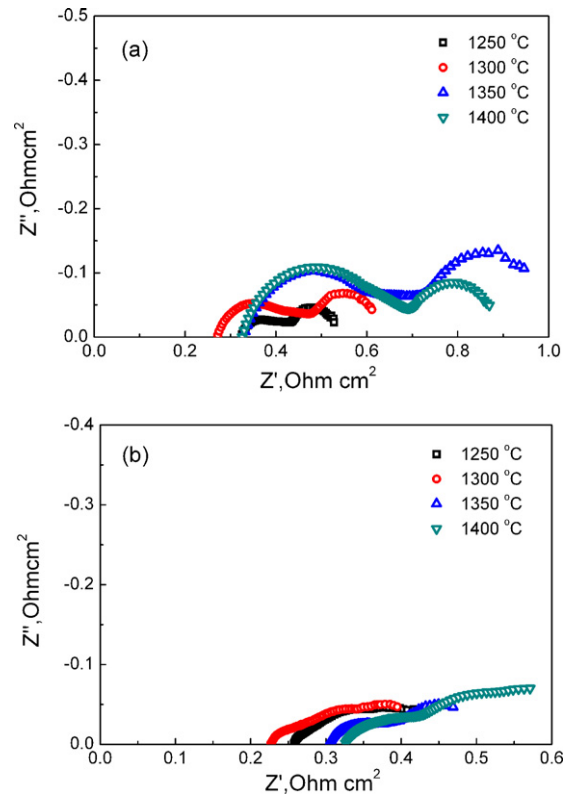


Fig. 8. The impedance plots of the fuel cell obtained at 650 °C. (a) NiO-Fe₂O₃/YSZ anode tube supported, (b) NiO-Fe₂O₃/GDC anode tube supported.

of the cell prepared at 1250 °C, respectively. It is because that the active surface area of catalysts became small in the case of the cells prepared at high co-sintering temperature. Small active area of catalyst particles finally increased the high frequency impedance arc. It is worth nothing that GDC based cells hold smaller overpotential resistance than that of YSZ based fuel cell. This is because that GDC itself also can be used as catalyst to increasing the rate of electrochemical reaction. The results again agreed that the accumulated pore volume of /GDC fuel cells is larger than that of its counterpart, which can be clearly seen in Figs. 4(a) and 5(a).

4. Summary

For NiO-Fe₂O₃-GDC, NiO-Fe₂O₃-YSZ tubular cells, the co-sintering temperature apparently affected the densification of electrolyte (or OCV) and the porosity of anode tube. The densification of the electrolyte is near to be completed at a sintering temperature of 1400 °C, while the porosity of anode becomes small as the co-sintering temperature increasing. The OCV of the cells is linearly related to the tube diameter shrinkage degree. It reaches 1.1 V which basically equals to the Nernst voltage prepared at 1400 °C. In both two types of fuel cells, the reducing value of accumulated pore volume sintered at 1400 °C is nearly 50% of that of the tube sintered at 1250 °C. Considering the pores provide place where fuel gases diffused and a large surface area of catalyst particles will increase the rate of the electrochemical reaction, the porosity of the anode tubes relying on the co-sintering temperature decide the power density fuel cells (with the same electrolyte and cathode). 1300 °C is the marginal temperature to obtain sufficient electrocatalytic activity of electrodes, and a higher temperature is needed to suppress gas leakage through the electrolyte.

Acknowledgement

This work is supported by Japan-US clean energy technologies development.

References

- [1] N.Q. Minh, *J. Am. Ceram. Soc.* 76 (1993) 563–588.
- [2] O. Yamamoto, *Electrochim. Acta* 45 (2000) 2423–2435.
- [3] S.C. Singhal, *Solid State Ionics* 152–153 (2002) 405–410.
- [4] B.C.H. Steele, A. Heinzel, *Nature* 414 (2001) 345–352.
- [5] S.C. Singhal, K. Kendall, *High Temperature Solid Oxide Fuel Cell: Fundamentals, Design and Applications*, Elsevier Limited, Oxford, UK, 2003.
- [6] Y. Funahashi, T. Shimamori, T. Suzuki, Y. Fujishiro, M. Awano, *J. Power Sources* 163 (2007) 731–736.
- [7] S. Livermore, J. Cotton, R. Ormerod, *J. Power Sources* 86 (2000) 411–416.
- [8] M. Masashi, H. Yoshiko, N.M. Sammes, *Solid State Ionics* 135 (2000) 743–748.
- [9] H.S. Noh, J.W. Son, H. Lee, H.S. Song, H.W. Lee, J.H. Lee, *J. Electrochem. Soc.* 156 (2009) B1484–B1490.
- [10] A. Bieberle-Hutter, D. Beckel, A. Infortuna, P.U. Muecke, *J. Power Sources* 177 (2008) 123–130.
- [11] A. Evans, A. Bieberle-Hutter, L.M.R. Jennifer, J.G. Ludwig, *J. Power Sources* 194 (2009) 119–129.
- [12] N.M. Sammes, Y. Du, R. Bove, *J. Power Sources* 145 (2005) 428–434.
- [13] K. Kendall, M. Palin, *J. Power Sources* 71 (1998) 268–270.
- [14] K. Yashiro, N. Yamada, T. Kawada, J. Hong, A. Kaimai, Y. Nigara, J. Mizusaki, *Electrochemistry* 70 (2002) 958–960.
- [15] T. Suzuki, M.H. Zahir, Y. Funahashi, T. Yamaguchi, Y. Fujishiro, M. Awano, *Electrochem. Commun.* 10 (2008) 1563–1566.
- [16] T. Suzuki, Y. Funahashi, T. Yamaguchi, Y. Fujishiro, M. Awano, *Electrochem. Solid-State Lett.* 10 (2007) A177–A179.
- [17] T. Suzuki, Y. Funahashi, T. Yamaguchi, Y. Fujishiro, M. Awano, *J. Electrochem. Soc.* 156 (2009) B318–B321.
- [18] T. Suzuki, M.H. Zahir, Y. Funahashi, T. Yamaguchi, Y. Fujishiro, M. Awano, *Science* 325 (2009) 852–855.
- [19] T. Ishihara, J.W. Yan, M. Shinagawa, H. Matsumoto, *Electrochim. Acta* 52 (2006) 1645–1650.
- [20] T. Ishihara, Y. Tsuruta, T. Todaka, H. Nishiguchi, Y. Takita, *Solid State Ionics* 153 (2002) 709–714.
- [21] J.W. Yan, M. Enoki, H. Matsumoto, T. Ishihara, *Electrochem. Solid-State Lett.* 10 (2007) B139–B141.
- [22] Y.W. Jua, H. Etob, T. Inagakic, S. Iida, T. Ishihara, *J. Power Sources* 195 (2010) 6294–6300.
- [23] Y. Funahashi, T. Shimamori, T. Suzuki, Y. Fujishiro, M. Awano, *ECS Trans.* 7 (2007) 643–649.
- [24] T. Yamaguchi, T. Suzuki, S. Shimizu, Y. Fujishiro, M. Awano, *J. Membr. Sci.* 300 (2007) 45–50.
- [25] S.B. Adler, *Solid State Ionics* 111 (1998) 125–134.
- [26] T. Suzuki, T. Yamaguchi, K. Hamamoto, Y. Fujishiro, M. Awano, N. Sammes, *Energy Environ. Sci.* 4 (2011) 940–943.